Inorganic Chemistry
Article

Inorg. Chem. **2010**, *49*, 11395–11402 **11395**
DOI: 10.1021/ic1014187

Insights into Metal Borohydride and Aluminohydride Bonding: X-Ray and Neutron Diffraction Structures and a DFT and Charge Density Study of [Na(15-crown-5)][EH_4] (E = B, Al)

Peter Sirsch,*,† Natascha L. N. Clark,† Lenuţa Onuţ,† Richard P. L. Burchell,† Andreas Decken,† G. Sean McGrady,*,† Aziz Daoud-Aladine,‡ and Matthias J. Gutmann‡

†*Department of Chemistry, University of New Brunswick, Fredericton, New Brunswick, Canada E3B 5A3, and* ‡*ISIS Neutron Facility, CCLRC Rutherford Appleton Laboratory, Chilton, Didcot, Oxfordshire OX11 0QX, UK*

Received July 15, 2010

The neutron and X-ray structures of [Na(15-crown-5)][BH_4] and [Na(15-crown-5)][AlH_4], respectively, are reported, along with a topological analysis of their DFT-computed charge densities that explores the bonding between the anionic complex hydride $[EH_4]^-$ (E=B, Al) and the counterion $[Na(15\text{-crown-5})]^+$. In each case, the interaction is weak and mainly electrostatic in nature; however, notable differences are observed in the manner in which $[BH_4]^-$ and $[AlH_4]^-$ bind to the metal, which explains their different coordination modes. A range of unconventional E−H···H−C contacts is revealed to play an important role in the overall bonding and crystal packing of both complexes. These interactions can be classified as weak dihydrogen bonds based on the *atoms in molecules* approach.

Introduction

Transition metal tetrahydroborato complexes[1,2] and their f-block analogs[3,4] have attracted considerable interest over recent decades as simple model systems for the activation of small ligands by metals. A deeper understanding of the structures and bonding displayed by these systems will afford insights into the nature of metal-mediated hydride transfer processes, which have both academic and industrial importance. Whereas in f-element complexes ionic contributions dominate the bonding between the metal (M) and the tetrahydroborate, $[BH_4]^-$, ligand,[4] the interaction in corresponding d-metal complexes is proposed to be largely covalent.[2,5] Numerous structural and theoretical studies have shown that the $[BH_4]^-$ moiety can interact with a transition metal in an η^1, η^2, or η^3 fashion through three-center B−H−M bonds, where the $[BH_4]^-$ group acts as a two-, four-, or six-electron donor, respectively, provided that metal orbitals of appropriate symmetry and energy are available.[5]

Alkali metal−crown ether cations also provide an acidic center to which $[BH_4]^-$ has been shown to coordinate in either a dihapto or trihapto fashion.[6,7] In contrast to d- and f-metal complexes, however, the nature of the interaction and hapticity preferences between $[BH_4]^-$ and alkali metal cations are largely unexplored. A recent computational study employing MO and NBO schemes investigated the bonding between $[BH_4]^-$ and Li^+ in a number of lithium amine complexes.[8] The authors concluded that in these systems the interaction is predominantly ionic in nature; however, a significant covalent contribution was found for η^2-coordinated $[BH_4]^-$.

We wished to investigate in further detail how the tetrahydroborate ligand interacts with a main group metal by carrying out a neutron diffraction study of [Na(15-crown-5)][BH_4] (**1**), accompanied by a topological analysis of its electron density, as derived from DFT calculations. This complex was recently characterized by X-ray diffraction, and significantly different distances were reported for its terminal and bridging B−H bonds, which implies that the interaction of the $[BH_4]^-$ moiety with the metal cation is more than just electrostatic in nature.[7] However, hydrogen atom positions obtained through X-ray diffraction are always approximate, which hinders definitive conclusions about the bonding. The

*To whom correspondence should be addressed. E-mail: psirsch@unb.ca (P.S.), smcgrady@unb.ca (G.S.M.).

(1) Marks, T. J.; Kolb, J. R. *Chem. Rev.* **1977**, *77*, 263.
(2) (a) Parry, R. W.; Kodama, G. *Coord. Chem. Rev.* **1993**, *128*, 245. (b) Xu, Z.; Lin, Z. *Coord. Chem. Rev.* **1996**, *156*, 139.
(3) Ephritikhine, M. *Chem. Rev.* **1997**, *97*, 2193.
(4) Arliguie, T.; Belkhiri, L.; Bouaoud, S.-E.; Thuery, P.; Villiers, C.; Boucekkine, A.; Ephritikhine, M. *Inorg. Chem.* **2009**, *48*, 221.
(5) Lledos, A.; Duran, M.; Jean, Y.; Volatron, F. *Inorg. Chem.* **1991**, *30*, 4440.
(6) (a) Gorbunov, A. I.; Storozhenko, P. A.; Ivakina, L. V.; Bulychev, B. M.; Gusev, A. I. *Dokl. Akad. Nauk. SSSR* **1985**, *285*, 129. (b) Antsyshkina, A. S.; Sadikov, G. G.; Porai-Koshits, M. A.; Konoplev, V. N.; Silina, T. A.; Sizareva, A. S. *Koord. Khim.* **1994**, *20*, 274.
(7) Gálvez Ruiz, J. C.; Nöth, H.; Warchhold, M. *Eur. J. Inorg. Chem.* **2008**, 251.
(8) Gálvez Ruiz, J. C.; Sanchez, M. *THEOCHEM* **2007**, *818*, 23.

Published on Web 11/19/2010

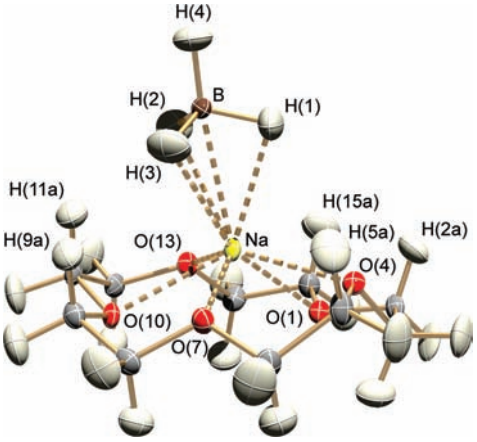

Figure 1. Molecular structure of [Na(15-crown-5)][BH_4], **1**, as determined by neutron diffraction at 100 K.

neutron structure of **1** reported here provides the first precise structural data for the hydrogen atoms involved in the B−H−M interaction and represents the first example of an alkali metal tetrahydroborato complex characterized by this technique. The nature of the bonding was further investigated by a theoretical charge density study of **1**. We were particularly interested to discover whether the boron atom participates in the bonding to the metal, and if so to what extent. Our analysis of complex **1** is complemented by a theoretical charge density study of the analogous tetrahydroaluminato complex [Na(15-crown-5)][AlH_4] (**2**), whose X-ray structure is also reported here. In contrast to the large numbers of transition metal tetrahydroborato complexes that have been structurally characterized to date, no experimental structures have been reported in which $[AlH_4]^-$ binds to a d- or f-block metal. Complex **2**, which has been reported before only as a private communication to the Cambridge Structural Database (CSD), remains the only characterized example to date where the $[AlH_4]^-$ moiety coordinates to a metal center.[9] A comparative study of the bonding in **1** and **2** therefore offers a unique opportunity to explore in detail how main group metals interact with simple group 13 hydride anions, and how this coordination perturbs the structure and internal electron distribution of the $[EH_4]^-$ (E = B, Al) moieties.

Results and Discussion

Neutron and X-Ray Diffraction Structures. The structure of **1** as determined by single crystal neutron diffraction at 100 K is shown in Figure 1; selected bond distances and angles are listed in Table 1. The $[BH_4]^-$ ligand coordinates to the sodium cation in an η^3 fashion with a Na···B distance of 2.600(6) Å. For comparison, a Na···B distance of 3.0654(1) Å is reported for $NaBH_4$, which adopts a structure isomorphous with NaCl,[10] and the sum of the van der Waals radii for Na and B is 3.4 Å.[11] Assuming an ionic radius of 1.18 Å for Na^+,[12] the observed Na···B distance is in agreement with a correlation reported by Edelstein between the M···B distance and the metal ion radius for complexes with η^3 M−BH_4 interactions.[13]

Table 1. Selected Bond Distances (Å) and Angles (deg) for the Neutron Structure of [Na(15-crown-5)][BH_4] **1** and Its DFT-Calculated Structure **1a**

moiety	neutron	DFT
B−Na	2.600(6)	2.469
B−H(1)	1.229(9)	1.232
B−H(2)	1.221(7)	1.239
B−H(3)	1.234(8)	1.240
B−H(4)	1.220(8)	1.210
Na−O	2.395(6)−2.501(5)	2.457−2.585
Na−H(1)	2.381(9)	2.395
Na−H(2)	2.454(9)	2.292
Na−H(3)	2.571(9)	2.344
H(2)···H(11a)	2.464(9)	3.661[a]
H(3)···H(9a)	2.505(10)	2.646, 2.283[a,b]
H(1)···H(5a)	3.437(12)	2.968[a]
H(2)···H(15a)	4.044(12)	3.029[a]
H(1)−B−H(4)	108.7(6)	111.01
H(2)−B−H(4)	110.5(5)	110.26
H(3)−B−H(4)	110.5(6)	110.13
H(1)−B−H(2)	108.1(6)	108.82
H(2)−B−H(3)	109.1(6)	108.27
H(1)−B−H(3)	109.8(6)	108.28
Na−B−H(4)	173.8(4)	176.73

[a] The coordination geometry for $[BH_4]^-$ changes in **1a** (c.f.). [b] Contact distances for H(3)···H(9a) and H(3)···H(11a), respectively.

As can be seen in Figure 1, the $[BH_4]^-$ moiety in **1** displays close-to-tetrahedral symmetry but is noticeably canted from the normal; this is reflected in a Na···B−H(4) angle of 173.8(4)°. As a result, $[BH_4]^-$ binds to the sodium cation in an asymmetric manner, with Na···H distances ranging from 2.381(9) to 2.571(9) Å. These values are comparable with the Na···H distance in NaH (2.445 Å)[14] but are slightly greater than the average Na···H distance of 2.337 Å observed for the bridging hydrogen atoms in [Na(15-crown-5)][$W(PMe_3)_3H_5$] (**3**), the only other complex reported so far, for which Na···H(bridge) contacts have been characterized by neutron diffraction.[15] The sodium cation in **3** is also coordinated in an asymmetric way by three W−H bonds, and a degree of covalent Na···H−W bonding was suggested by the authors. The interaction with the complex anion in **3** pulls the sodium cation some 1.10 Å out of the least-squares plane defined by the five oxygen atoms of the crown ether ring, a displacement only slightly larger than the 1.041(5) Å observed here for **1**.

In contrast to its X-ray structure,[7] the neutron structure of **1** shows no significant differences between the lengths of the bridging and terminal B−H bonds: all four B−H distances are identical within the range of error [1.220(8)−1.234(8) Å]. A similar situation was reported for **3**, with average W−H(terminal) = 1.775 and W−H(bridge) = 1.770 Å distances deduced. In contrast, significantly extended B−H(bridge) bonds, as long as 1.290(9) Å, were observed in the neutron structures of the dihapto transition metal tetrahydroborato complexes [(η^5-$CH_3C_5H_4$)$_2$-Hf(η^2-BH_4)$_2$] (**4**)[16] and [Co(terpy)(η^2-BH_4)] (terpy = 2,2′:6′2″-terpyridine) (**5**).[17] While the four B−H distances in **1** are equal, they are somewhat longer than the terminal

(9) Trzaska, S.; Olbrich, F. Private communication, CSD refcode: PAPNOK, **2005**.
(10) Filinchuk, Y.; Hagemann, H. *Eur. J. Inorg. Chem.* **2008**, 3127.
(11) Bondi, A. *J. Phys. Chem.* **1964**, *68*, 441.
(12) Shannon, R. D. *Acta Crystallogr.* **1976**, *A32*, 751.
(13) Edelstein, N. *Inorg. Chem.* **1981**, *20*, 297.
(14) Shull, C. G.; Wollan, E. O.; Morton, G. A.; Davidson, W. L. *Phys. Rev.* **1948**, *73*, 842.
(15) Berry, A.; Green, M. L. H.; Bandy, J. A.; Prout, K. *J. Chem. Soc., Dalton Trans.* **1991**, 2185.
(16) Johnson, P. L.; Cohen, S. A.; Marks, T. J.; Williams, J. M. *J. Am. Chem. Soc.* **1978**, *100*, 2709.
(17) Corey, E. J.; Cooper, N. J.; Canning, W. M.; Lipscomb, W. N.; Koetzle, T. F. *Inorg. Chem.* **1982**, *21*, 192.

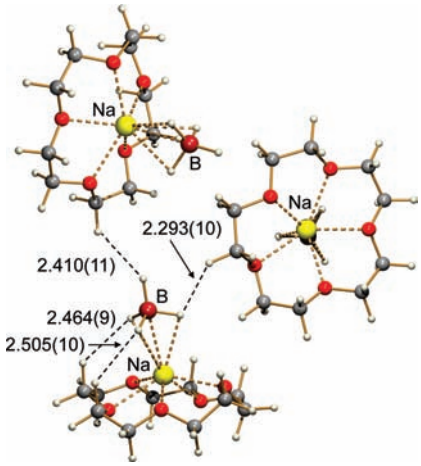

Figure 2. Selected inter- and supramolecular B−H···H−C interactions (distances in Å) revealed by the neutron diffraction structure of [Na(15-crown-5)][BH_4] (**1**). Only two of a total of five supramolecular contacts are shown.

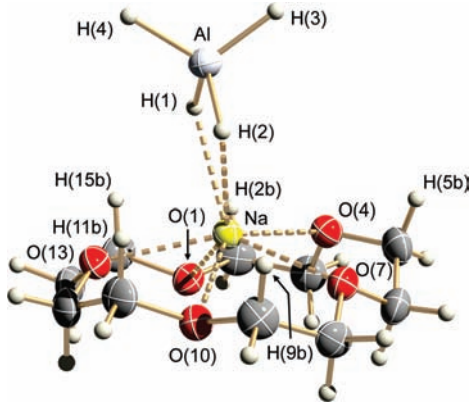

Figure 3. Molecular structure of [Na(15-crown-5)][AlH_4], **2**, as determined by X-ray diffraction at 173 K.

B−H bonds in **4** and **5**, with average distances of 1.192 and 1.216 Å, respectively. This elongation, as well as the tilting of the $[BH_4]^-$ moiety in **1**, can be rationalized by a multitude of inter- and supramolecular B−H···H−C interactions, which constitute an important contribution to the crystal packing in the three-dimensional structure of **1** (Figure 2). All four hydrogen atoms of $[BH_4]^-$ are involved in these unconventional hydrogen bonds[18] and a total of seven (two inter- and five supramolecular) B−H···H−C contacts are observed for each $[BH_4]^-$ moiety, with distances ranging from 2.293(10) to 2.505(10) Å.

A similar bonding pattern is also observed for the $[AlH_4]^-$ analog **2**, whose structure has been determined by X-ray diffraction (Figures 3 and 4; Table 2). Once again, all four hydrogen atoms of the $[AlH_4]^-$ moiety participate in Al−H···H−C interactions (two of them inter- and five supramolecular), with measured H···H contact distances in the range 2.43(5)−2.80(5) Å, slightly longer than the corresponding distances in **1** on account of the X-ray data used to characterize these distances for **2**. In contrast to the η^3-coordinating $[BH_4]^-$ ligand in **1**, the $[AlH_4]^-$ moiety in **2** binds to the sodium cation in an η^2 fashion, with a

(18) (a) Belkova, N. V.; Shubina, E. S.; Epstein, L. M. *Acc. Chem. Res.* **2005**, *38*, 624. (b) Custelcean, R.; Jackson, J. E. *Chem. Rev.* **2001**, *101*, 1963.

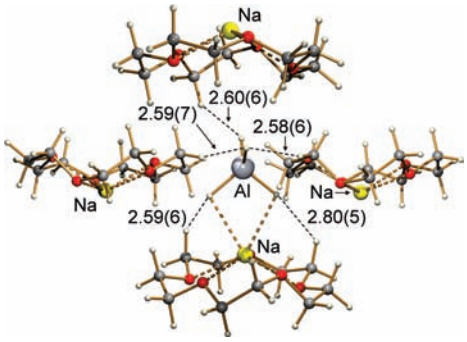

Figure 4. Selected inter- and supramolecular Al−H···H−C interactions (distances in Å) revealed by the X-ray diffraction structure of [Na(15-crown-5)][AlH_4], **2**. Only three of a total of five intermolecular contacts are shown.

Table 2. Selected Bond Distances (Å) and Angles (deg) for the X-Ray Structure of [Na(15-crown-5)][AlH_4] **2** and its DFT-Calculated Structure **2a**

moiety	X-ray	DFT
Al−Na	3.119(2)	3.005
Al−H(1)	1.55(4)	1.659
Al−H(2)	1.56(4)	1.665
Al−H(3)	1.53(5)	1.611
Al−H(4)	1.58(5)	1.616
Na−O	2.407(2)−2.425(2)	2.439−2.554
Na−H(1)	2.43(3)	2.345
Na−H(2)	2.45(5)	2.291
H(1)···H(15b)	2.80(5)	2.493
H(1)···H(2b)	3.34(5)	2.887
H(2)···H(11b)	2.59(6)	2.469
H(2)···H(9b)	2.80(6)	2.598
H(1)−Al−H(2)	101(2)	98.89
H(3)−Al−H(4)	113(3)	115.83
H(1)−Al−H(3)	109(2)	110.86
H(1)−Al−H(4)	110(2)	109.93
H(2)−Al−H(3)	111(2)	110.27
H(2)−Al−H(4)	113(2)	108.90

Na···Al distance of 3.119(2) Å (sum of van der Waals radii: 3.92 Å). The interaction draws the sodium cation out of the least-squares plane of the crown ether oxygen atoms by 0.754(1) Å. Although the hydrogen atom positions in **2** are only approximate, it is clear that the $[AlH_4]^-$ moiety deviates from regular tetrahedral symmetry: the angle H(1)−Al−H(2), of 101(2)°, which involves the two bridging hydrogen atoms, is smaller than tetrahedral, and H(3)−Al−H(4), which defines the terminal, is measured at 113(6)°. This trend is confirmed by the DFT calculations for **2**, which indicate a difference of around 17° in these two angles. As with the $[BH_4]^-$ ligand in **1**, $[AlH_4]^-$ also adopts an asymmetric position atop the sodium-crown ether cation, albeit less pronounced than in **1**. The X-ray distances of 2.43(3) and 2.45(5) Å measured for the two Al−H···Na contacts suggest that the interactions between Na and the two bridging H atoms is at least of comparable strength to the Na···H−B interactions in **1**.

DFT Structures. The DFT geometries we obtained for **1** and **2** (henceforth denoted as **1a** and **2a**) are in very good agreement with the experimental neutron and X-ray structure, respectively (Tables 1 and 2), bearing in mind that in the X-ray structure of **2** all distances involving hydrogen atoms are systematically foreshortened. Only the Na···E (E = B, Al) and the respective Na···H distances are significantly shorter in the calculated structures. This is most easily explained by the fact that significant intermolecular

interactions in the solid state are not accounted for in the gas phase DFT models of the molecular ion pairs. Thus, the $[EH_4]^-$ groups in **1a** and **2a** interact with only one [Na(15-crown-5)]$^+$ cation, instead of participating in a range of additional E−H···H−C interactions as observed in the crystal structures of **1** and **2** (Figures 2 and 4).

Our DFT optimizations confirm that η^3 and η^2 coordination are the most stable binding modes for $[BH_4]^-$ and $[AlH_4]^-$, respectively. Notably, the $[EH_4]^-$ groups in **1a** and **2a** adopt tilted and nonsymmetric positions above the sodium−crown ether cation (see Figure 7 and the Supporting Information for details), as observed experimentally in the neutron (**1**) and X-ray (**2**) structures. Short E−H···H−C contacts in both systems (see Tables 1 and 2) are indicative of intermolecular unconventional hydrogen bonds, attesting to the significance of these interactions that we ascribe to the experimental structures of **1** and **2**. It is noteworthy that the coordination geometry of the $[BH_4]^-$ moiety calculated for **1a** is considerably different from the experimental geometry measured for **1**: The $[BH_4]^-$ group in **1a** is rotated by ca. 60° relative to the experimental structure, which allows one of its hydride moieties to form simultaneous B−H···H−C interactions with two C−H bonds of the crown ether ring. In the neutron structure of **1**, these same two C−H bonds are interacting instead with two different B−H moieties from a neighboring $[BH_4]^-$ unit. The potential energy surface characterizing in-place rotation of the η^3-$[BH_4]^-$ moiety in **1a** is very flat, and reorientation of $[BH_4]^-$ can be achieved with no significant energy penalty: The energy difference between the optimized structure **1a** and one with the same $[BH_4]^-$ orientation as in the neutron structure of **1** has been calculated to be less than 14 kJ/mol. It is thus unsurprising that a different coordination is adopted in the crystalline form of **1**.

Comparison of the calculated structures **1a** and **2a** with their experimental counterparts reveals another noteworthy feature: the distances of the bridging E−H bonds in the DFT structures are significantly longer than their terminal counterparts, as might be expected on account of their coordination to the sodium cation. In the neutron structure of **1**, however, all B−H bonds were identical within the range of experimental error, and the DFT results indicate that all experimental bonds are slightly elongated. Furthermore, comparison of the calculated and experimental structures reveals that it is not solely the coordination of $[EH_4]^-$ to sodium that induces asymmetry in the structure and bonding of the group 13 anions; this is a result also of the additional inter- and supramolecular E−H···H−C interactions observed in the experimental structures of **1** and **2**. Intra- and intermolecular B−H···H−C interactions have been reported before for aminoboron hydrides and azacyclohexane−borane adducts,[18b,19] as well as very recently for a number of lithium tetrahydroborate complexes with aromatic amines.[20] The strengths of dihydrogen bonds of the form B−H···H−X (X = N, O) in systems containing

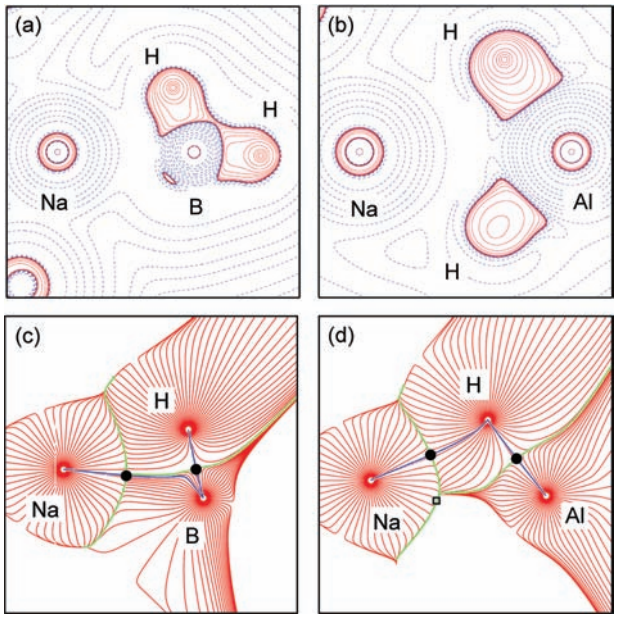

Figure 5. (a, b) Contour plots of the negative Laplacian, $-\nabla^2\rho(\mathbf{r})$, in the Na−E−H (E = B, Al) plane of **1a** and **2a**, respectively. Solid and dashed lines represent charge concentration and depletion, respectively. (c, d) Gradient vector field, $\nabla\rho(\mathbf{r})$, in the same planes as a and b; bond paths are indicated by blue lines, BCPs by closed circles.

$[BH_4]^-$ have been estimated to range from 10 to 27 kJ/mol.[21] These secondary interactions are important and have a measurable impact on the structures of **1** and **2**, also because of their number and because the overall strength of the Na···$[EH_4]^-$ interaction is relatively weak: The binding energies we obtained for **1a** and **2a** with respect to the isolated ions are 365.4 and 329.4 kJ/mol, respectively.

In the following, we turn our attention to the nature of the bonding between $[EH_4]^-$ and the sodium cation, which we have explored through a topological analysis of the electron densities of **1a** and **2a** using the "atoms in molecules" approach.[22] This discloses in detail how the sodium cation interacts with the group 13 hydride anions, revealing significantly different bonding scenarios for **1** and **2**.

Charge Density Studies. Figure 5 shows the Laplacian and the gradient vector field of the electron density, $\rho(\mathbf{r})$, for **1a** and **2a** in a map containing sodium, boron and aluminum, respectively, and at least one of the bridging hydrogen atoms. The topology of $\rho(\mathbf{r})$ is remarkably different in the two cases: in **1a**, a bond path connects Na and B, whereas in **2a** it is the bridging H atom that interacts with Na, and not the Al atom. The topological parameters at the bond critical points (BCPs) of the bond paths are listed in Table 3. They reveal that the interaction between Na and B in **1a**, as well as that between Na and the bridging H atoms in **2a**, is weak and electrostatic in nature: ρ(BCP) in these bonds is relatively small and $\nabla^2\rho$(BCP) is clearly positive, and the value of ρ(BCP) suggests a bond strength comparable to medium to strong hydrogen bonds.[23] This conclusion is also supported by the AIM charges, obtained by integrating the electron density

(19) (a) Padilla-Martínez, I. I.; Rosales-Hoz, M. J.; Tlahuext, H.; Camacho-Camacho, C.; Ariza-Castolo, A.; Contreras, R. *Chem. Ber.* **1996**, *129*, 441. (b) Flores-Parra, A.; Sánchez-Ruiz, S. A.; Guadarrama, C.; Nöth, H.; Contreras, R. *Eur. J. Inorg. Chem.* **1999**, 2069.

(20) Aguilar-Martínez, M.; Félix-Baéz, G.; Pérez-Martínez, C.; Nöth, H.; Flores-Parra, A.; Colorado, R.; Galvez-Ruiz, J. C. *Eur. J. Inorg. Chem.* **2010**, 1973.

(21) Epstein, L. M.; Shubina, E. S.; Bakhmutova, E. V.; Saitkulova, L. N.; Bakhmutov, V. I.; Chistyakov, A. L.; Stankevich, I. V. *Inorg. Chem.* **1998**, *37*, 3013.

(22) Bader, R. F. W. *Atoms in Molecules: A Quantum Theory*; Oxford University Press: Oxford, U.K., 1990.

Table 3. Selected Topological Parameters for the Theoretical Electron Densities of **1a** and **2a** [$\rho(\mathbf{r})$ in e/Å^3; $\nabla^2\rho(\mathbf{r})$ in e/Å^5]

moiety	ρ(BCP)	$\nabla^2\rho$(BCP)	ε	δ
		[Na(15-crown-5)][BH_4] (**1a**)		
Na−B	0.118	2.086	1.10	0.03
B−H(1)	1.000	−1.148	0.05	0.54
B−H(2)	0.977	−0.667	0.05	0.53
B−H(3)	0.966	−0.369	0.05	0.52
B−H(4)	1.080	−3.065	0.01	0.57
Na···H(1)[a]				0.03
Na···H(2)[a]				0.05
Na···H(3)[a]				0.04
H(3)···H(9a)	0.030	0.277	0.09	0.02
H(3)···H(11a)	0.053	0.433	0.06	0.04
H(2)···H(15a)	0.015	0.145	0.35	0.01
Na−O	0.076−0.099	1.484−2.091	0.03−0.07	0.04−0.05
		[Na(15-crown-5)][AlH_4] (**2a**)		
Na···Al[a]				0.01
Al−H(1)	0.438	5.189	0.03	0.32
Al−H(2)	0.430	5.120	0.03	0.31
Al−H(3)	0.497	5.915	0.00	0.39
Al−H(4)	0.491	5.823	0.00	0.39
Na···H(1)	0.086	1.226	0.65	0.06
Na···H(2)	0.094	1.359	0.41	0.07
H(1)···H(2b)	0.022	0.223	0.36	0.02
H(1)···H(15b)	0.042	0.349	0.08	0.03
H(2)···H(9b)	0.035	0.301	0.06	0.03
H(2)···H(11b)	0.045	0.380	0.04	0.03
Na−O	0.083−0.103	1.617−2.216	0.01−0.08	0.04−0.05

[a] No bond path observed between these atoms.

Table 4. AIM Charges of Selected Atoms in **1a** and **2a**[a]

	1a (E = B)	**2a** (E = Al)
Na	+0.89 [+0.90]	+0.89 [+0.90]
E	+1.67 [+1.66]	+2.23 [+2.22]
H(1)	−0.65 [−0.67]	−0.78 [−0.81]
H(2)	−0.65 [−0.67]	−0.79 [−0.81]
H(3)	−0.65 [−0.67]	−0.77 [−0.81]
H(4)	−0.62 [−0.67]	−0.78 [−0.81]
$\sum(EH_4)$	−0.90 [−1.00]	−0.89 [−1.00]
O	−1.05... −1.06 [−1.06]	−1.05... −1.06 [−1.06]
H(11a)/H(11b)	+0.06 [+0.02]	+0.05 [+0.02]
H(9a)/H(9b)	+0.05 [+0.02]	+0.05 [+0.02]
H(15a)/H(15b)	+0.04 [+0.02]	+0.05 [+0.03]
H(5a)/H(5b)	+0.06 [+0.03]	+0.05 [+0.05]
H(2a)/H(2b)	+0.03 [+0.03]	+0.04 [+0.03]

[a] Values in square brackets denote atomic charges prior to the coordination of $[EH_4]^-$ to $[Na(15\text{-crown-5})]^+$.

over the respective atomic basins. As can be seen in Table 4, the atomic charges in $[EH_4]^-$ do not change significantly upon coordination to $[Na(15\text{-crown-5})]^+$; the net charge transfer from the anion to the cation is only ca. 0.1 electron. It is noteworthy, however, that all bridging E−H bonds are markedly weaker than their terminal counterparts (by more than 10%), which is not reflected to the same extent in the differences in their bond lengths.

The bond ellipticity ε, a measure of the deviation from σ symmetry, is noticeably high at the Na···B BCP in **1a** and at the Na···H BCPs in **2a**. This indicates that $\rho(\mathbf{r})$ is not only small, but also diffuse in these regions. In cases of such delocalized bonding, the delocalization index δ(A,B),

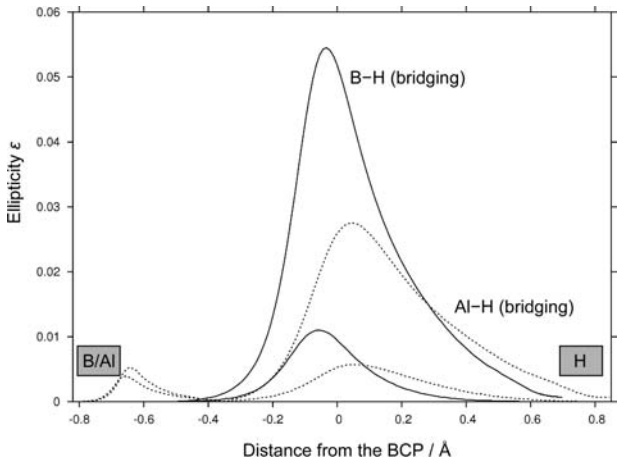

Figure 6. Comparison of the ellipticity ε along the E−H bond paths for bridging and terminal hydrogen atoms in **1a** and **2a**. B−H bonds are represented by solid lines, Al−H bonds by dashed lines.

which measures the number of electron pairs shared between two atoms A and B,[24] offers a more appropriate metric than bond paths to track the various bonding contributions. On the basis of the values of δ in Table 3, there are comparable bonding interactions in **1a** between Na and both B and the bridging H atoms [δ(Na,B) = 0.03; δ(Na,H) = 0.03−0.05]. It appears that Na has no clear preference to interact exclusively with B, and binds to the B−H moiety as a whole. The situation in **2a**, on the other hand, is clearly different: here, the value of δ(Na,Al) is negligible and more than six times smaller than δ(Na,H) for the two Na−H bonds [δ(Al,H) = 0.009 vs δ(Na,H) = 0.06]. The bonding between Na and $[AlH_4]^-$ is therefore contained exclusively in the Na···H interactions, and Al does not participate in the interaction. This is also reflected in the gradient vector field of **2a** (Figure 5d), which shows that Na and Al do not share a larger interatomic surface area, in contrast to Na and B in **1a** (Figure 5c).

The difference in bonding between **1a** and **2a** is in accord with the significantly different natures of B−H and Al−H bonds, as revealed by the topological analysis. Thus, all bridging B−H bonds exhibit clear covalent character [indicated by a high ρ(BCP), negative $\nabla^2\rho$(BCP), and large δ(B,H)], with significant electron density concentrated in the region between the atoms. The highly Lewis-acidic sodium cation then interacts with the B−H moiety as a whole, causing the electron density in this bond to polarize toward Na, in a manner reminiscent of σ-bond complexation.[25] This polarization is revealed by tracing ε, the ellipticity of $\rho(\mathbf{r})$, along the respective B−H bond paths. Figure 6 clearly shows that the bridging B−H bond displays a measurably greater deviation from σ symmetry than does the terminal one, a direct consequence of the attractive interaction with the sodium cation.

Al−H bonds, on the other hand, are far more ionic in nature, as indicated by lower electron density than for B−H bonds, a positive Laplacian, and a smaller δ(Al,H)

(23) (a) Koch, U; Popelier, P. L. A. *J. Phys. Chem.* **1995**, *99*, 9747. (b) Braga, D.; Grepioni, F.; Desiraju, G. R. *Chem. Rev.* **1998**, *98*, 1375.

(24) Fradera, X.; Austen, M. A.; Bader, R. F. W. *J. Phys. Chem. A* **1999**, *103*, 304.

(25) (a) Kubas, G. J. *Metal Dihydrogen and σ-Bond Complexes: Structure, Theory and Reactivity*; Kluwer Academic/Plenum Publishers: New York, 2001. (b) Kubas, G. J. *J. Organomet. Chem.* **2001**, *635*, 37. (c) Crabtree, R. H. *Angew. Chem., Int. Ed. Engl.* **1993**, *32*, 789.

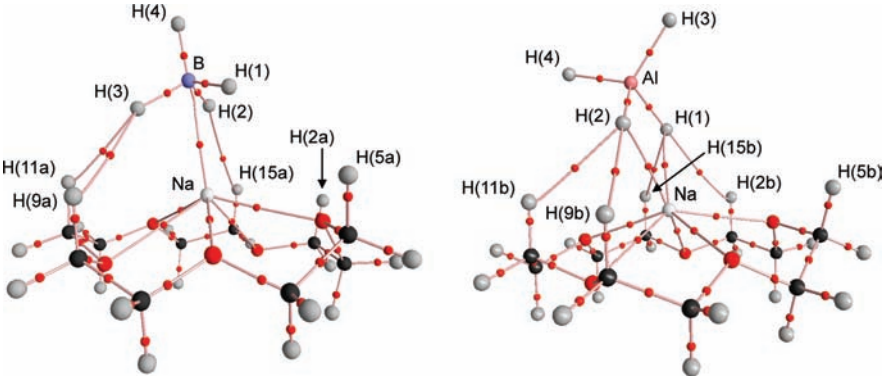

Figure 7. Complete set of bond paths for **1a** (left) and **2a** (right). BCPs are represented by red circles.

(Table 3). A higher negative charge now resides on the hydrogen atoms (Table 4), and considerably less electron density is located in the Al−H bonds. As a consequence, the sodium cation interacts almost exclusively with the bridging hydrogen atoms, and the polarization of $\rho(\mathbf{r})$ in the Al−H bonds is far less pronounced (Figure 6). Coordination in an η^2 fashion is now more favorable than is η^3, since it allows the bridging H atoms to approach the metal cation more closely, to maximize the electrostatic Na···H interactions. The observed deviation of the $[AlH_4]^-$ moiety from ideal tetrahedral symmetry, with a relatively small H(1)−Al−H(2) angle (X-ray, 101.2°; DFT, 98.9°), supports this interpretation and implies that the Na···H interactions in **2** are more important than is the Na···Al one.

Finally, Figure 7 depicts a complete set of bond paths for **1a** and **2a** and shows that the aforementioned E−H···H−C interactions are also characterized by bond paths in $\rho(\mathbf{r})$. These H···H interactions are highly intriguing, as they lie between the extremes of established dihydrogen bonds[26] and the more recently recognized hydrogen−hydrogen bonds.[27] Such interactions have not been investigated in detail using the AIM approach. Whereas dihydrogen bonds are characterized by electrostatic and directional interactions between hydrogen atoms that carry opposite charges of significant magnitude,[26a] the term hydrogen−hydrogen bonding has been suggested for stabilizing interactions between hydrogen atoms which carry very small charges and often of the same sign, as for example in C−H···H−C interactions.[27]

The atomic charges obtained for the respective hydrogen atoms in **1a** and **2a** (Table 4) confirm the electrostatic nature of the H···H interactions in both systems. The acidic H atoms carry a significant positive charge, which is greater than those of the other hydrogen atoms in the crown ether ring (charges of the H atoms not listed in Table 4 range between −0.01 and +0.01 in **1a**, and between 0.00 and +0.01 in **2a**). In contrast, H atoms involved in hydrogen−hydrogen bonding usually acquire additional electron density and carry charges that are less positive (or more negative) than in the unperturbed molecule.[27b] It is noteworthy that H(5a) in **1a** also bears a higher than average positive charge, which indicates that this atom might be involved in dihydrogen bonding with the nearest hydridic H atom (d[H(1)···H(5a)] = 2.97 Å), in spite of the absence of a bond path. H(2a) in **1a** and H(5b) in **2a** also carry significant positive charges; however, in contrast to H(5a), these do not change upon coordination of $[EH_4]^-$, and the distances to nearby E−H moieties also rule out any significant H···H interactions.

The topological parameters at the BCPs of the H···H bond paths (Table 3) indicate that dihydrogen bonding in both **1a** and **2a** is comparatively weak.[28] This is in accord with the small degree of destabilization observed for the acidic H atoms: compared to $[Na(15\text{-crown-}5)]^+$, their atomic energies rise by 13.1−39.4 kJ/mol in **1a** [39.4 H(11a), 25.5 H(9a), 14.2 H(15a), 13.1 kJ/mol H(5a)] and 16.6−38.0 kJ/mol in **2a** [38.0 H(11b), 25.6 H(9b), 34.5 H(15b), 16.6 kJ/mol H(2b)], which is markedly less than the H atom destabilization reported in systems with intermediate-to-strong dihydrogen bonds (84−167 kJ/mol).[27]

Although H(15a) and H(5a) in **1a** are very similar in terms of their atomic charges, destabilization energies, and distances to nearby B−H moieties (see Table 1), a H···H bond path is observed only for H(15a) and not for H(5a). This can be rationalized by the topology of the electron density in these regions. The topological parameters at the H···H BCPs, along with the destabilization energies, clearly show that the dihydrogen bonding in **1a** is strongest in the bifurcated H···H interaction between H(3) and H(9a)/H(11a). The interaction between H(2) and H(15a), in comparison, is considerably weaker, and the high ellipticity at the corresponding BCP reveals that the electron density is not only very small but also flat in that region. Furthermore, $\rho(\mathbf{r})$ at the nearest ring critical point (RCP; 0.45 Å away; an RCP is a minimum in $\rho(\mathbf{r})$ in two dimensions) is only negligibly lower (by 0.001 e/Å^3) than at the BCP. These observations indicate a high degree of instability: such bonds can easily be ruptured as a consequence of slight structural changes or alterations in the electron density.[28,29] Hence, it is likely that the absence of

(26) (a) Crabtree, R. H. *Science* **1998**, *282*, 2000. (b) Stevens, R. C.; Bau, R.; Milstein, R.; Blum, O.; Koetzle, T. F. *J. Chem. Soc., Dalton Trans.* **1990**, 1429. (c) Lough, A. L.; Park, S.; Ramachandran, R.; Morris, R. H. *J. Am. Chem. Soc.* **1994**, *116*, 8356. (d) Richardson, T. B.; de Gala, S.; Crabtree, R. H. *J. Am. Chem. Soc.* **1995**, *117*, 12875.

(27) (a) Matta, C. F.; Hernández-Trujillo, J.; Tang, T.-H.; Bader, R. F. W. *Chem.—Eur. J.* **2003**, *9*, 1940. (b) Matta, C. F. In *Hydrogen Bonding − New Insights* (*Challenges and Advances in Computational Chemistry and Physics Series*); Grabowski, S. J., Ed.; Springer: Dordrecht, The Netherlands, 2006; Chapter 9.

(28) Popelier, P. L. A. *J. Phys. Chem.* **1998**, *102*, 1873.

(29) (a) Cremer, D.; Kraka, E.; Slee, T. S.; Bader, R. F. W.; Lau, C. D. H.; Nguyen-Dang, T. T.; MacDougall, P. J. *J. Am. Chem. Soc.* **1983**, *105*, 5069. (b) Bader, R. F. W.; Matta, C. F. *Organometallics* **2004**, *23*, 6253.

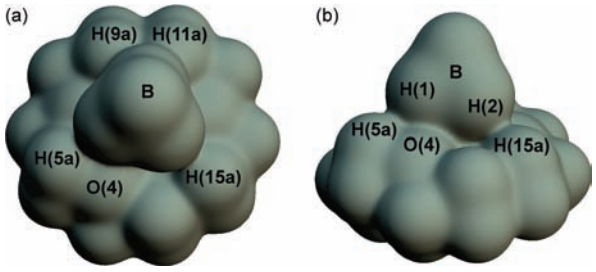

Figure 8. 3D envelope maps of the electron density of **1a** for $\rho(\mathbf{r}) = 0.01$ e/Å^3. (a) Top view, (b) side view.

an analogous bond path between H(1) and H(5a) in **1a** is a consequence of the specific folding of the crown ether ring, which places the electron density of the oxygen atom O(4) in close proximity to the acidic hydrogen atom H(5a) (see Figure 8). This serves to flatten the electron density in this region even further and inhibits the formation of a stable bond path between H(5a) and H(1).

Conclusions

The structure and bonding adopted by complexes formed between the anionic group 13 hydrides $[EH_4]^-$ (E = B, Al) and the sodium-crown ether cation $[Na(15\text{-crown-}5)]^+$ have been explored by a combination of neutron and X-ray diffraction studies and the analysis of DFT-computed electron densities. The neutron and X-ray structures of $[Na(15\text{-crown-}5)][\eta^3\text{-}(BH_4)]$ (**1**) and $[Na(15\text{-crown-}5)][\eta^2\text{-}(AlH_4)]$ (**2**), respectively, reveal that the $[EH_4]^-$ group in both cases is notably canted from the normal and coordinates to Na^+ in an asymmetric manner; furthermore, all four B−H bonds in **1** are significantly elongated. These observations can be rationalized by a multitude of short inter- and supramolecular E−H···H−C contacts which are present in the crystal structures of both **1** and **2**. On the basis of the topological analysis of the electron density, these interactions can be classified as weak dihydrogen bonds. Although intrinsically weak, a multiplicity of unconventional hydrogen bonds can exert an important influence on the structure adopted in the solid state,[23b] and these interactions apparently play an important role in the crystal structures adopted by **1** and **2**.

The bonding between the $[EH_4]^-$ moieties and Na^+ has been further analyzed by AIM methods and shown to be weak and electrostatic in nature. This agrees with the neutron structure of **1**, in which the lengths of the bridging and terminal B−H bonds are revealed to be identical within the range of error, in contrast to an earlier reported X-ray structure. The topological analysis of the electron densities demonstrates that the different coordination modes of $[BH_4]^-$ (tridentate) and $[AlH_4]^-$ (bidentate) are accompanied by markedly different bonding scenarios. These can be rationalized by the significant difference in size and electronegativity between B and Al: The difference in electronegativity renders the B−H bonds more covalent and less polar than their Al−H counterparts, which in turn causes the sodium cation to interact solely with the hydrogen atoms in the case of bridging Al−H moieties. B−H bonds, on the other hand, bind to Na^+ as a whole, in a manner reminiscent of σ-type complexation. In this case, the smaller size of boron allows three rather than two B−H moieties to approach the cationic metal center without compromising the important Na···B interaction.

Table 5. Crystallographic Data for $[Na(15\text{-crown-}5)][BH_4]$ (**1**) and $[Na(15\text{-crown-}5)][AlH_4]$ (**2**)

compound	**1**	**2**
chemical formula	$C_{10}H_{24}BNaO_5$	$C_{10}H_{24}AlNaO_5$
M_r	258.09	274.26
space group	$P2_12_12_1$	$P2_1/c$
a/Å	7.7751(17)	9.7904(18)
b/Å	11.519(2)	10.2580(18)
c/Å	16.058(4)	15.926(3)
α/deg	90	90
β/deg	90	97.395(3)
γ/deg	90	90
V/Å^3	1438.2(5)	1586.2(5)
Z	4	4
radiation	neutron	X-ray
λ (Å)	0.35−10.0	0.71073
T/K	100(2)	173(2)
D_c/g cm^{-3}	1.192	1.148
μ/mm^{-1}	$0.57102 + 0.1198\lambda$	0.161
reflns collected	6329	10418
unique reflections	1787	3527
$R_1{}^a$ (observed), wR_2(all)^b	0.0758/0.1895	0.0615/0.1876
GOF^c	1.039	1.099

$^a R_1 = \sum||F_o| - |F_c||/\sum|F_o|$. $^b wR_2 = \{\sum[w(F_o^2 - F_c^2)^2]/\sum[w(F_o^2)^2]\}^{1/2}$. ^{c}GOF $= [\sum w(F_o^2 - F_c^2)^2/(n_o - n_p)]^{1/2}$.

Experimental Section

Syntheses were carried out using standard Schlenk and inert atmosphere techniques. All reagents were purchased from Sigma-Aldrich. $NaBH_4$ and $NaAlH_4$ were used without further purification. 15-crown-5 ether was dried before use by dissolving in THF and storing the resulting solution over dried molecular sieves (5 Å). THF was purified and dried prior to use.

Synthesis of [Na(15-crown-5)][BH$_4$] (1). A mixture of $NaBH_4$ (0.075 g; 2.0 mmol), a 2 M solution of 15-crown-5 ether in THF (1.0 mL; 2.0 mmol), and THF (20.0 mL) was stirred for 4 h under an Ar atmosphere. All solids were removed by filtration. The filtrate was transferred to a Schlenk tube and stored at 5 °C. Colorless crystals were obtained after 2 days. Elemental analysis calculated for $C_{10}H_{24}BNaO_5$: C, 46.51%; H, 7.75%; B, 4.26%. Found: C, 46.19%; H, 9.78%; B, 3.25%. ^{1}H NMR (THF-d_8, 300 MHz, 298 K): 2.4 (s, 20H, crown), [−0.8−(−0.3)] (q, 4H, $[BH_4]^-$). ^{11}B NMR (THF-d_8, 97 MHz, 298 K): [−43.7−(−40.4)], (qn, 4H, $[BH_4]^-$, $^1J_{BH} = 77$ Hz).

Synthesis of [Na(15-crown-5)][AlH$_4$] (2). A mixture of $NaAlH_4$ (0.75 g; 13.8 mmol), a 2 M solution of 15-crown-5 ether in THF (8.0 mL; 16.0 mmol), and THF (20.0 mL) was stirred for 4 h under an Ar atmosphere. All solids were removed by filtration. The filtrate was transferred to a Schlenk tube and stored at 5 °C. Colorless crystals were obtained after 2 days. Elemental analysis calculated for $C_{10}H_{24}AlNaO_5$: C, 43.79%; H, 8.75%; Al, 9.85%. Found: C, 41.81%; H, 8.61%; Al, 9.54%. ^{1}H NMR (THF-d_8, 300 MHz, 298 K): 3.7 (s, 20H, crown), 3.4−3.2 (q, 4H, $[AlH_4]^-$). ^{27}Al (THF-d_8, 79 MHz, 298 K): 93.2−102.1 (qn, 4H, $[AlH_4]^-$, $^1J_{BH} = 173$ Hz).

Neutron Diffraction Study of 1. A large suitable single crystal of dimensions 5 × 1 × 1 mm was selected in a glovebox, fixed in a glass capillary with perfluorinated polyether, and mounted on the SXD diffractometer at the ISIS spallation neutron source (Rutherford Appleton Laboratories, Oxfordshire, U.K.). SXD uses the time-of-flight Laue technique to obtain reflections from large amounts of reciprocal space in a single measurement with a stationary crystal.[30] Data were collected at 100 K from six crystal orientations to a resolution of 0.2445 Å, each experiment taking around 33 h (last one 30 h), giving a total data collection

(30) (a) Wilson, C. C. *Z. Kristallogr.* **2005**, *220*, 385. (b) Keen, D. A.; Gutmann, M. J.; Wilson, C. C. *J. Appl. Crystallogr.* **2006**, *39*, 714.

time of just over 8 days. The program SXD-2001 was used to collect and process the diffraction data; absorption effects were corrected numerically.[31] The initial atomic coordinates for the heavy atoms were taken from a previously determined X-ray structure, and the neutron scattering lengths were taken to be b_c(C) = 6.646, b_c(H) = −3.739, b_c(B) = 5.30, b_c(Na) = 3.63, and b_c(O) = 5.803 fm.[32] During the refinement, difference Fourier maps clearly revealed all of the hydrogen atom positions, and all atoms of the asymmetric unit were refined anisotropically using SHELXL.[33] Further details of the refinements and crystallographic data are listed in Table 5. Plots were generated using the programs ORTEP-3[34] and PLUTON.[35] A further description of the crystallographic model can be retrieved from the respective CIF file, available as Supporting Information.

X-Ray Diffraction Study of 2. A suitable single crystal of dimensions 0.30 × 0.30 × 0.20 mm was coated with paratone-N oil, mounted using a glass fiber, and frozen in the cold nitrogen stream of a goniometer. A hemisphere of data was collected on a Bruker AXS P4/SMART 1000 diffractometer using graphite monochromated Mo Kα radiation (λ = 0.71073 Å) and ω and θ scans with a scan width of 0.3°. The unit cell parameters were obtained by least-squares refinement of 4690 reflections. Raw data were integrated with the program SAINT,[36] and corrections for absorption effects were applied using SADABS.[37] The structure was solved by a combination of direct methods (SHELXS)[38] and iterative difference-Fourier syntheses (SHELXTL).[39] All non-hydrogen atoms were refined anisotropically. Hydrogen atoms were found in Fourier difference maps and refined isotropically. The number of refined parameters was 250. The maximum residual electron density was 0.50 and the minimum was −0.31 eÅ^{-3}. Further details of the refinements and crystallographic data are listed in Table 5. A further description of the crystallographic model can be retrieved from the respective CIF file, available as Supporting Information.

Computational Details. DFT calculations were performed with the Gaussian 09 program suite[40] using the B3LYP density functional,[41] along with the implemented 6-311G(d,p) basis set.[42] All geometry optimizations were carried out without imposing any symmetry constraints, except $[BH_4]^-$ and $[AlH_4]^-$, which were optimized in T_d symmetry. The structures reported here were confirmed as true minima on the respective potential energy surface by calculating analytical frequencies. The topology of the electron density was analyzed using the software packages AIMPAC,[43] AIMALL,[44] and AIM2000.[45] The atomic energies reported for the acidic hydrogen atoms were estimated by multiplying their atomic kinetic energies by the factor $-(\gamma - 1)$ with $\gamma = -V/T$, as described, e.g., in ref 27a. The value of the molecular virial ratio γ deviated from 2 by less than 3.8×10^{-3} in all optimized systems.

Acknowledgment. We thank the Natural Sciences and Engineering Research Council of Canada and the Canada Foundation for Innovation for financial support of this work and the Atlantic Computational Excellence Network (ACEnet) for providing computing facilities. The neutron diffraction study of **1** at the ISIS Pulsed Neutron and Muon Source was supported by a beam time allocation from the Science and Technology Facilities Council. We are indebted to Dr. Chérif F. Matta for his helpful suggestions and comments.

Supporting Information Available: Crystallographic data for **1** and **2** in CIF format. Cartesian coordinates and geometrical parameters for all model systems. This material is available free of charge via the Internet at http://pubs.acs.org.

(31) Gutmann, M. J.; Wilson, C. C. *SXD-2001*; ISIS, Rutherford Appleton Laboratories: Oxfordshire, England, 2001.
(32) Sears, V. F. *Neutron News* **1992**, *3*, 26.
(33) Sheldrick, G. M. *SHELXL-97*; University of Göttingen: Göttingen, Germany, 1997.
(34) Farrugia, L. J. *J. Appl. Crystallogr.* **1997**, *30*, 565.
(35) Spek, A. L. *PLATON*; Utrecht University: Utrecht, The Netherlands, 2010.
(36) *SAINT 7.23A*; Bruker AXS, Inc.: Madison, WI, 2006.
(37) Sheldrick, G. M. *SADABS*; Bruker AXS, Inc.: Madison, WI, 2004.
(38) Sheldrick, G. M. *SHELXS*; University of Göttingen: Göttingen, Germany, 2001.
(39) Sheldrick, G. M. *SHELXTL*; University of Göttingen: Göttingen, Germany, 2001.
(40) Frisch, M. J.; Trucks, G. W.; Schlegel, H. B.; Scuseria, G. E.; Robb, M. A.; Cheeseman, J. R.; Scalmani, G.; Barone, V.; Mennucci, B.; Petersson, G. A.; Nakatsuji, H.; Caricato, M.; Li, X.; Hratchian, H. P.; Izmaylov, A. F.; Bloino, J.; Zheng, G.; Sonnenberg, J. L.; Hada, M.; Ehara, M.; Toyota, K.; Fukuda, R.; Hasegawa, J.; Ishida, M.; Nakajima, T.; Honda, Y.; Kitao, O.; Nakai, H.; Vreven, T.; Montgomery, J. A., Jr.; Peralta, J. E.; Ogliaro, F.; Bearpark, M.; Heyd, J. J.; Brothers, E.; Kudin, K. N.; Staroverov, V. N.; Kobayashi, R.; Normand, J.; Raghavachari, K.; Rendell, A.; Burant, J. C.; Iyengar, S. S.; Tomasi, J.; Cossi, M.; Rega, N.; Millam, J. M.; Klene, M.; Knox, J. E.; Cross, J. B.; Bakken, V.; Adamo, C.; Jaramillo, J.; Gomperts, R.; Stratmann, R. E.; Yazyev, O.; Austin, A. J.; Cammi, R.; Pomelli, C.; Ochterski, J. W.; Martin, R. L.; Morokuma, K.; Zakrzewski, V. G.; Voth, G. A.; Salvador, P.; Dannenberg, J. J.; Dapprich, S.; Daniels, A. D.; Farkas, O.; Foresman, J. B.; Ortiz, J. V.; Cioslowski, J.; Fox, D. J. *Gaussian 09*, Revision A.02; Gaussian, Inc.: Wallingford, CT, 2009.
(41) (a) Becke, A. D. *J. Chem. Phys.* **1993**, *98*, 5648. (b) Lee, C.; Yang, W.; Parr, R. G. *Phys. Rev. B* **1988**, *37*, 785. (c) Miehlich, B.; Savin, A.; Stoll, H.; Preuss, H. *Chem. Phys. Lett.* **1989**, *157*, 200.
(42) (a) McLean, A. D.; Chandler, G. S. *J. Chem. Phys.* **1980**, *72*, 5639. (b) Krishnan, R.; Binkley, J. S.; Seeger, R.; Pople, J. A. *J. Chem. Phys.* **1980**, *72*, 650. (c) Wachters, A. J. H. *J. Chem. Phys.* **1970**, *52*, 1033. (d) Hay, P. J. *J. Chem. Phys.* **1977**, *66*, 4377. (e) Raghavachari, K.; Trucks, G. W. *J. Chem. Phys.* **1989**, *91*, 1062.
(43) (a) Biegler-König, F. W.; Bader, R. F. W.; Tang, T. *J. Comput. Chem.* **1982**, *3*, 317. (b) Cheeseman, J. R.; Keith, T. A.; Bader, R. F. W. *AIMPAC program package*; McMaster University: Ontario, Canada, 1997.
(44) Keith, T. A. *AIMALL*, version 09.04.23; TK Gristmill Software: 2009.
(45) (a) Biegler-König, F. W.; Schönbohm, J. *J. Comput. Chem.* **2000**, *21*, 1040. (b) Biegler-König, F. W.; Schönbohm, J. *J. Comput. Chem.* **2002**, *23*, 1489.